

Cite this: *New J. Chem.*, 2012, **36**, 2033–2041

www.rsc.org/njc

PAPER

Synthesis, X-ray crystal structures, optical properties and modelling data of neutral bis(1,2-dithiolene) nickel complexes of the “non-cyclic SR” family†

Thanh-Tuan Bui,^{ab} Minh Ha Vuong,^{ab} Bénédicte Garreau-de Bonneval,^{ab} Fabienne Alary,^c Jacob Kane,^{ab} Carine Duhayon,^{ab} Alix Sournia-Saquet^{ab} and Kathleen I. Moineau-Chane-Ching^{*ab}

Received (in Victoria, Australia) 16th May 2012, Accepted 13th July 2012

DOI: 10.1039/c2nj40398f

Three nickel-bisdithiolene-based compounds were synthesized and characterized by X-ray single crystal (for two of them), electrochemical and spectroscopic analyses. A minor change in the alkyl chain structure surrounding the nickel-bisdithiolene core induces dramatic changes in molecular packing: **complex 1** crystallizes in a triclinic ($P\bar{1}$) space group while **complex 3** crystallizes in a monoclinic ($C2/c$) space group. No such differences are to be noted concerning electrochemical or spectroscopic characteristics, the alkyl chains induce no influence on electronic parameters. Furthermore, theoretical calculations were conducted to obtain theoretical insight of the behaviour of the complexes. The three complexes were investigated by DFT calculations using the PBE0 functional.

Introduction

During the past decade, electron accepting small molecules have attracted considerable attention due to a number of promising applications in organic electronics: organic field-effect transistors,¹ light emitting diodes,² and sensors.³ In the field of organic photovoltaics (OPV), different classes of electron accepting small molecules have been explored. The fullerene derivatives, and especially [6,6]-phenyl-C₆₁-butyric acid methyl ester (PCBM), are the most studied ones.⁴ In general, a drawback of employing PCBM for organic photovoltaics is that it absorbs poorly in the visible part of the solar spectrum.⁵ Other organic small molecules have been emerging recently as an attractive alternative to fullerenes due to the ease of tuning their band structure by chemical modifications: perylenes, vinazenes, diketopyrrolopyrroles and benzothiadiazoles gave rise to promising results.⁶ Previously, we have reported on tetra-phenyl substituted nickel bisdithiolene complexes.⁷ They are efficient electron acceptors and give rise

to different ways of packing in the condensed state – crystalline or liquid crystalline phases – depending on the nature and position of functional groups grafted on the molecule periphery.⁸

Regarding the other known electron accepting small molecules, neutral square planar nickel organic complexes constitute a promising class of molecules for OPV applications: (i) they absorb strongly in the vis-NIR region of the solar spectrum, (ii) they present a great stability towards oxygen, water or relatively high temperatures (at least up to 350 °C), (iii) their neutral character is essential for such applications. Moreover, some of them exhibit a π -stacked columnar structure with a remarkably high electron mobility of 2.8 cm² V⁻¹.⁹ All these specificities confirm their interest for organic electronics. The key step in the development of such molecules for such applications involves developing structure–property relationships for tuning their absorption, their electronic properties or their physical properties. In that aim, and in the continuation of our former work, we focus on the rational design of nickel bisdithiolenes: we investigate here three derivatives possessing alkyl chains grafted on the dithiolene core. They are part of the family commonly known as the “non-cyclic SR family”¹⁰ (Fig. 1). The pendant alkyl chains introduced in the periphery of the molecule may influence the way of packing which therefore significantly differs from that of complexes with cyclic ligands.¹¹ To the best of our knowledge, crystallographic data of molecules with odd-numbered chain lengths are presented here for the first time.

In addition to this experimental contribution, theoretical investigations are carried out in parallel to fully describe these

^a CNRS, LCC (Laboratoire de Chimie de Coordination), 205, route de Narbonne, BP 44099, F-31077 Toulouse, France

^b Université de Toulouse, UPS, INPT, LCC, F-31077 Toulouse, France. E-mail: kathleen.chane@lcc-toulouse.fr; Tel: +33 5 61 33 31 52

^c CNRS, IRSAMC, Laboratoire de chimie et physique quantiques, 118 route de Narbonne, F-31062 Toulouse, France

† Electronic supplementary information (ESI) available: X-Ray structures, schemes and computed RAMAN data. CCDC 646782 (for **complex 1**) and CCDC 646783 (for **complex 3**). For ESI and crystallographic data in CIF or other electronic format see DOI: 10.1039/c2nj40398f

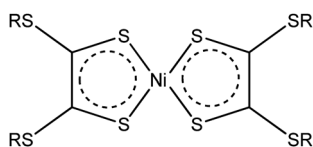


Fig. 1 General structure of neutral bis-dithiolene complexes of the SR family.

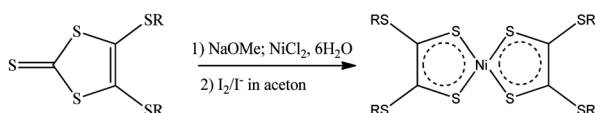
complexes: in recent work,¹² we have shown by using a reliable model system that DFT calculations provide high quality calculations of structural parameters and vibrational spectra. On the contrary, computation of absorption spectra of such nickel dithiolene molecules needs elaborate multireference approaches to achieve accurate results in the reproduction of the very intense electronic transition displayed by these sets of complexes in the UV-VIS-NIR region. The multideterminantal character of the ground state wave function prohibits use of DFT calculations and the size of the complexes investigated in this work renders *ab initio* studies unrealistic. On the one hand, we performed DFT calculations to explore the incidence of large alkyl chains on the Raman spectra of Ni(dmit)₂ (dmit²⁻ = 2-thioxo-1,3-dithiole-4,5-dithiolato) derivatives. On the other hand, theoretical calculations are performed and systematically compared to experimental results concerning parameters of the molecular structures, energy levels HOMO and LUMO, electronic and Raman scattering.

Results and discussion

Scheme 1 illustrates the final step of the synthesis of the three complexes. The preparation of the bis(alkylthio)-substituted 1,3-dithiole-2-thione precursors **ligands 1 to 3** was carried out according to a published procedure¹³ but with optimized reflux times and purification by column chromatography instead of recrystallization, allowing a quantitative yield to be systematically reached. Subsequent **complexes 1 to 3** were obtained with improved yields (33, 69 and 62%, respectively) in comparison to the reference procedure (15%), thanks to longer times of stirring and refluxing. While **complexes 1 and 3** were obtained as dark green crystals, **complex 2** was isolated as a viscous oil.

Crystal structure descriptions

X-ray-quality crystals of **complex 1** and **complex 3** were grown by slow evaporation from dichloromethane–methanol solutions. The molecular structures were analyzed by X-ray structural analysis at 160 K and 150 K, respectively. As previously described for parent compounds containing linear alkyl chains [Ni(S₂C₂(SC₄H₉)₂)₂] (**complex A**) and [Ni(S₂C₂(SC₆H₁₃)₂)₂] (**complex B**),¹³ **complex 1**



ligand 1: R1 = C₇H₁₅, *n*-heptyl
ligand 2: R2 = C₈H₁₇, 2-ethylhexyl
ligand 3: R3 = C₅H₁₁, 2-methylbutyl

complex 1: [Ni(S₂C₂(SC₇H₁₅)₂)₂]
complex 2: [Ni(S₂C₂(SC₈H₁₇)₂)₂]
complex 3: [Ni(S₂C₂(SC₅H₁₁)₂)₂]

Scheme 1 Schematic synthetic path leading from **ligands 1–3** to **complexes 1–3**.

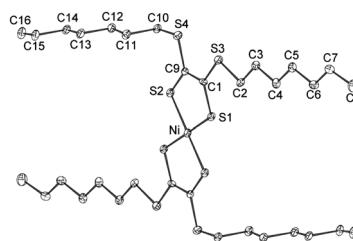


Fig. 2 Molecular structure of **complex 1** and numbering scheme. Thermal displacement ellipsoids are drawn at the 50% probability level.

crystallizes in a triclinic system *c*, space group *P* $\bar{1}$, with one molecule per unit cell (the Ni atom lies in a centre of symmetry and thus the asymmetric unit contains half a molecule). Fig. 2 displays the molecular structure of **complex 1**.

The central [Ni(S₂C₂S₂)₂] core of the molecule is planar (the maximum deviation from the mean plane is 0.09 Å for atom C9). The C2–C8 side chain is almost located in the plane of this central core, their two respective planes forming a dihedral angle of 8.41°. Conversely the C10–C16 side chain is significantly twisted as its mean plane makes a dihedral angle of 87.38° with the plane of the central core (a side view of the molecule is given in Fig. S1 (ESI[†])). Measured bond lengths and angles of **complex 1** are listed in Table 1. For comparison and subsequent discussion, computed values are also gathered in Table 1.

Since the unit cell contains only one molecule, the crystal structure is a simple periodic pattern in which the molecules are repeated by the parameters *a*, *b*, *c*. The overall packing can be described as a set of columns of molecules running along the [100] axis (Fig. 3). The shortest distance between two adjacent Ni atoms is thus the *a* parameter (5.335 Å), but since the molecules are strongly tilted with respect to this direction, the distance between two [Ni(S₂C₂S₂)₂] mean planes is 3.66 Å. There is no molecular overlap and no short contacts.

Complex 3 crystallises in the monoclinic system, space group *C2/c*. As for **complex 1**, the molecule [Ni(S₂C₂(SC₄H₉)₂)₂] is centrosymmetric with the Ni atom lying on a centre of symmetry (Fig. 4).

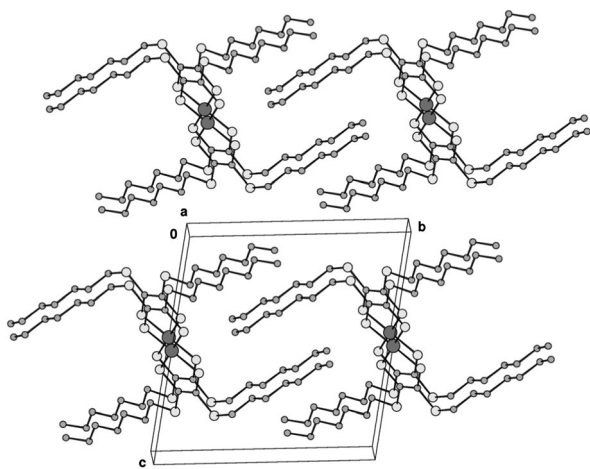
The central [Ni(S₂C₂S₂)₂] core is planar, the C2–C6 side chain lies at the central plane while the C8–C12 side chain is much more twisted (a side view of the molecule is given in Fig. S2 (ESI[†])). Bond lengths and angles are reported in Table 2. For comparison and subsequent discussion, computed values are also gathered in Table 2.

The molecules are stacked in columns along the [010] direction, the shortest distance between two Ni atoms is so the *b* parameter (6.464 Å). As the central plane [Ni(S₂C₂S₂)₂] of the molecules is strongly tilted with regard to the [010] direction, the shortest distance between two repeated [Ni(S₂C₂S₂)₂] planes in a column is 3.75 Å. As before, owing to this arrangement in the crystal, there is no short contact or molecular overlap (Fig. 5).

In a previous study,¹³ it has been observed that the melting points of parent linear-chain-containing complexes fluctuate depending on the odd or even number of carbons constituting the chain. The following explanation was tentatively proposed: the alkyl chains influence the interaction between the [Ni(S₂C₂S₂)₂] cores. In order to assess this hypothesis, we compare crystallographic data

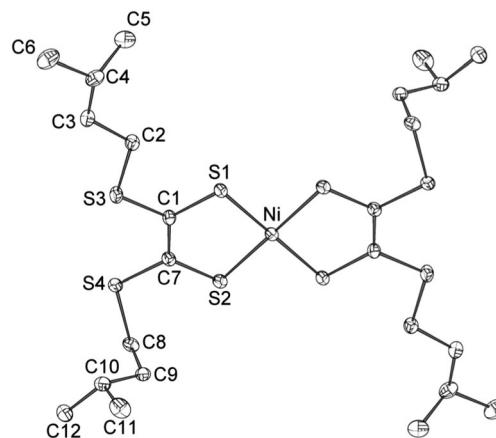
Table 1 Comparative experimental (X-ray) and computed values of bond lengths (Å) and angles (°) for **complex 1**

	Distance			Distance	
	Experimental	Computed		Experimental	Computed
S ₁ –Ni	2.1207(13)	2.131	C ₄ –C ₅	1.509(8)	1.521
S ₁ –C ₁	1.712(5)	1.710	C ₅ –C ₆	1.517(7)	1.521
S ₃ –Ni	2.1319(13)	2.133	C ₆ –C ₇	1.503(8)	1.521
S ₂ –C ₉	1.699(5)	1.710	C ₇ –C ₈	1.512(8)	1.519
S ₃ –C ₁	1.743(5)	1.757	C ₁₀ –C ₁₁	1.520(7)	1.522
S ₃ –C ₂	1.799(5)	1.821	C ₁₁ –C ₁₂	1.518(7)	1.518
S ₄ –C ₉	1.752(5)	1.761	C ₁₂ –C ₁₃	1.516(7)	1.521
S ₄ –C ₁₀	1.810(5)	1.820	C ₁₃ –C ₁₄	1.512(7)	1.521
C ₁ –C ₉	1.368(7)	1.398	C ₁₄ –C ₁₅	1.519(7)	1.521
C ₂ –C ₃	1.511(7)	1.519	C ₁₅ –C ₁₆	1.514(8)	1.519
C ₃ –C ₄	1.523(7)	1.522			
Angle		Angle		Angle	
	Experimental	Computed		Experimental	Computed
S ₁ –Ni–S ₂	91.94(5)	92.1	C ₃ –C ₄ –C ₅	114.0(5)	113.2
S ₁ –C ₁ –S ₃	120.8(3)	121.8	C ₄ –C ₅ –C ₆	113.4(5)	113.5
S ₁ –C ₁ –C ₉	119.2(4)	119.8	C ₅ –C ₆ –C ₇	113.8(5)	113.7
S ₂ –C ₉ –C ₁	120.1(4)	119.7	C ₉ –S ₂ –Ni	104.20(18)	104.3
S ₃ –C ₁ –C ₉	120.0(4)	118.4	C ₉ –S ₄ –C ₁₀	104.7(3)	103.8
S ₃ –C ₂ –C ₃	109.0(4)	109.0	C ₁₀ –C ₁₁ –C ₁₂	110.4(4)	112.0
S ₄ –C ₁₀ –C ₁₁	115.8(4)	114.5	C ₁₁ –C ₁₂ –C ₁₃	113.8(5)	113.1
C ₁ –S ₁ –Ni	104.48(19)	104.2	C ₁₂ –C ₁₃ –C ₁₄	113.7(5)	113.6
C ₁ –S ₃ –C ₂	103.9(3)	103.2	C ₁₃ –C ₁₄ –C ₁₅	113.4(4)	113.7
C ₂ –C ₃ –C ₄	111.5(5)	112.0	C ₁₄ –C ₁₅ –C ₁₆	113.1(5)	113.4

**Fig. 3** Perspective view of the packing of **complex 1** molecules.

previously reported for two of the studied complexes (**complex A** and **complex B**),¹³ with even-numbered chain lengths, with those of **complex 1** (see Table 3). The dihedral angles measured for the twisted chains are used to compare their deviations from the core plane: Φ_1 and Φ_2 are the S₂–C₉–S₄–C₁₀ and the C₉–S₄–C₁₀–C₁₁ dihedral angles, respectively, of **complex 1**. The same Φ_1 and Φ_2 angles were measured for **complexes A and B**. The shortest Ni–Ni distance and the distance between two adjacent [Ni(S₂C₂S₂)₂] mean planes may give information about possible central cores interactions. Data for **complex 3** are also reported in Table 3.

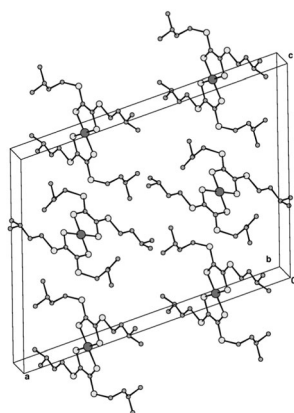
The three linear-chain-containing complexes crystallize in the *P* $\bar{1}$ space group and they show similar crystallographic data, in particular concerning the distance between [Ni(S₂C₂S₂)₂] mean planes, from 3.50 to 3.69 Å. No supplementary specific interaction through either Ni···S or S···S contact is formed in

**Fig. 4** X-Ray structure of **complex 3** showing the molecular unit and numbering scheme.

complex 1 if compared to **complex B**. There is thus no clear explanation for the rising of the melting point of **complex 1** (82 °C) in comparison to that of **complex B** (70 °C). For **complex B** and **complex 1**, the atomic deviation of the end-chain carbon relative to the [Ni(S₂C₂S₂)₂] mean plane is of the same order of magnitude (2.748 and 2.338 Å, respectively). It is noteworthy that the torsion of the chain occurs at the first carbon (C₁₀) of the chain for **complexes A and 1** whereas it is observed at the third one (C₁₂) for **complex B**. Thus, the fluctuation over a temperature range of 20 °C for the *n* = 4 to *n* = 11 derivatives observed by Underhill *et al.*¹³ probably relies on interactions between the alkyl chains. This is clearly the case for **complex 3** which presents a high melting point of 168 °C and for which numerous S···H short contacts between two adjacent molecules can be observed (see ESI†).

Table 2 Comparative experimental (X-ray) and computed values of bond lengths (Å) and angles (°) for **complex 3**

	Distance				
	X-Ray	Computed		X-Ray	Computed
S ₁ –Ni	2.1330(7)	2.133	C ₂ –C ₃	1.518(4)	1.529
S ₁ –C ₁	1.703(3)	1.700	C ₃ –C ₄	1.523(4)	1.529
S ₂ –Ni	2.1325(7)	2.132	C ₄ –C ₅	1.516(5)	1.523
S ₂ –C ₇	1.701(3)	1.700	C ₄ –C ₆	1.514(5)	1.522
S ₃ –C ₂	1.804(3)	1.804	C ₈ –C ₉	1.521(4)	1.521
S ₄ –C ₇	1.746(3)	1.743	C ₉ –C ₁₀	1.523(4)	1.527
S ₄ –C ₈	1.814(3)	1.807	C ₁₀ –C ₁₁	1.514(4)	1.522
C ₁ –C ₇	1.404(4)	1.400	C ₁₀ –C ₁₂	1.527(4)	1.523
Angle					
	X-Ray	Computed		X-Ray	Computed
S ₁ –Ni–S ₂	92.41(3)	92.0	C ₃ –C ₄ –C ₆	110.1(3)	109.88
S ₁ –C ₁ –S ₃	121.99(15)	122.0	C ₅ –C ₄ –C ₆	112.9(5)	110.6
S ₂ –C ₇ –S ₄	122.14(15)	122.8	C ₇ –S ₂ –Ni	104.46(9)	104.6
C ₁ –S ₁ –Ni	104.15(10)	104.5	C ₇ –S ₄ –C ₈	103.58(13)	104.1
C ₁ –S ₃ –C ₂	104.05(13)	130.4	C ₇ –C ₁ –S ₁	119.7(2)	119.6
C ₁ –C ₇ –S ₂	119.2(2)	119.3	C ₇ –C ₁ –S ₃	118.26(19)	118.4
C ₁ –C ₇ –S ₄	118.6(2)	117.9	C ₈ –C ₉ –C ₁₀	115.1(2)	115.9
C ₂ –C ₃ –C ₄	113.6(2)	113.6	C ₉ –C ₈ –S ₄	113.5(2)	115.1
C ₃ –C ₂ –S ₃	107.41(18)	108.5	C ₉ –C ₁₀ –C ₁₁	110.0(3)	109.9
C ₃ –C ₄ –C ₅	112.9(3)	112.4	C ₉ –C ₁₀ –C ₁₁	111.9(3)	109.9
			C ₁₁ –C ₁₀ –C ₁₂	110.5(3)	110.5

**Fig. 5** Perspective view of the packing of **complex 3** molecules.

Computed geometrical parameters

As can be seen in Tables 1 and 2, geometry optimizations lead to computed geometrical parameters in very good agreement with experimental data for the two complexes. The computed distances as well as the angles are very well reproduced. For the dithiolene core, the values of the C–C bond lengths as well as of the C–S bond lengths clearly indicate their delocalized character. Starting from

these results, we propose to describe the core of **complex 2** through computed structural parameters. They are collected after geometry optimisation without symmetry constraints in Fig. 6. The geometrical parameters proposed in Fig. 6 have expected values: the bonds lengths as well as the angles are comparable to those observed in the crystal structures of **complex 1** and **complex 2**.

Cyclic voltammetry

Electrochemistry of **complexes 1 and 2** has already been described,¹⁴ showing three electrochemical processes attributed to electron exchange on the core of the complexes. Table 4 reports the measured potential values associated with the first reduction and the first oxidation of **complexes 1 to 3**, respectively. A formula proposed by Brédas *et al.*¹⁵ on the basis of a comparison between effective Hamiltonian calculations and experimental electrochemical measurements on the conjugated system allows their HOMO and LUMO energy levels to be estimated.

$$\text{HOMO} = -(E_{1/2}(\text{ox}) + 4.8) \text{ eV and}$$

$$\text{LUMO} = -(E_{1/2}(\text{red}) + 4.8) \text{ eV}$$

They give rise to the value of the electrochemical bandgap denoted E_g^{el} . Experimental values are gathered in Table 4, and calculated values are included for comparison:

Table 3 Comparative data obtained by X-ray structural analysis on complexes containing either linear alkyl chains (**complexes A, B and 1**) or branched alkyl chains (**complex 3**)

	[Ni(S ₂ C ₂ (SC ₄ H ₉) ₂) ₂] Complex A^a	[Ni(S ₂ C ₂ (SC ₆ H ₁₃) ₂) ₂] Complex B^a	[Ni(S ₂ C ₂ (SC ₇ H ₁₅) ₂) ₂] Complex 1^b	[Ni(S ₂ C ₂ (SC ₅ H ₁₁) ₂) ₂] Complex 3^b
Space group	<i>P</i> $\bar{1}$	<i>P</i> $\bar{1}$	<i>P</i> $\bar{1}$	<i>C</i> 2/ <i>c</i>
Distance 1 ^c	<i>a</i> = 7.753 Å	<i>a</i> = 5.254 Å	<i>a</i> = 5.335 Å	<i>b</i> = 6.464 Å
Distance 2 ^d	3.69 Å	3.50 Å	3.66 Å	3.75 Å
ϕ_1^e	10.19°	2.07°	7.26°	21.09°
ϕ_2^e	79.93°	177.72°	83.62°	76.17°

^a Ref. 13. ^b This work. ^c Shortest Ni–Ni distance. ^d Distance between [Ni(S₂C₂S₂)] mean planes. ^e Defined in the text (see above).

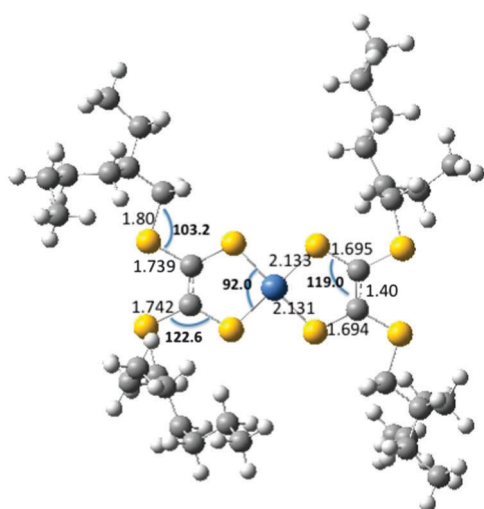


Fig. 6 Computed bond lengths (Å) and angles (°) for **complex 2**.

Table 4 Comparative experimental (electrochemistry) and computed values of the HOMO–LUMO bandgaps

Complex	Electrochemical data ^a					Computed data	
	$E^{1/2}$ (red)/V	$E^{1/2}$ (ox)/V	LUMO/eV	HOMO/eV	E_g^{el} /eV	LUMO/eV	HOMO/eV
1	-0.13	0.73	-4.67	-5.53	0.86	-3.42 (a _g)	-4.96(a _u)
2	-0.13	0.73	-4.67	-5.53	0.86	-3.42	-4.96
3	-0.14	0.74	-4.66	-5.54	0.88	-3.45(a _g)	-4.98(a _u)

^a Reduction and oxidation potentials (V/SCE) obtained by SQW in CH₂Cl₂ with (*n*-Bu₄)[PF₆] (0.1 mol L⁻¹) on Pt microdisk.

The electrochemical redox potentials are very similar for the three complexes. The eigenvalues of the computed HOMO–LUMO are in good agreement with the experimental ones: the computed HOMOs are around 0.6 eV lower in energy than the values deduced from electrochemistry. The difference for LUMO energies is slightly higher (around 1.3 eV). The calculated frontier orbitals of the three complexes are identical in shape and in energy (see Fig. S4 in the ESI†). HOMOs are ligand in character while the LUMOs are mainly S (3p) in character and display antibonding interactions with a 3d orbital of the nickel atom. Ligand valence orbitals lie at higher energy than the Ni-d orbital manifold. The different alkyl chains have no effect on the electronic properties of the three complexes. The electrochemical bandgaps (E_g^{el}) are found to be similar, around 0.9 eV whereas calculated values are found to be significantly larger: $E_g^{cal} = 1.53$ – 1.54 eV. It is worth noting that our calculations give the same value for the three molecules since the HOMO and LUMO energies are not affected by the presence of the different alkyl chains.

Electronic spectra

Neutral bis(1,2-dithiolene) complexes absorb strongly in the NIR region.^{16–18} This absorption is usually assigned to a π – π^* transition between orbitals delocalized over the [Ni(S₂C₂S₂)₂] core of the complex.^{9,19} As can be seen in Fig. 7, the electronic

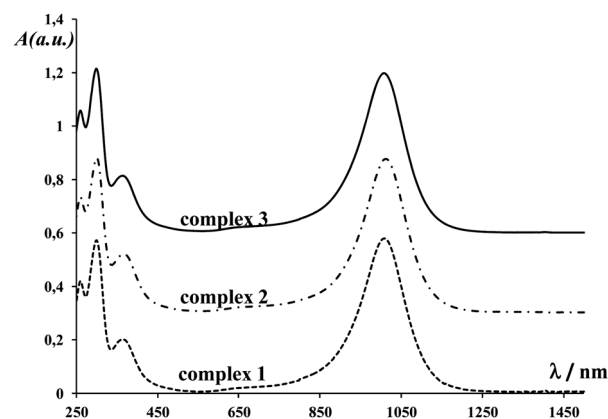


Fig. 7 Electronic spectra of **complex 1**, **complex 2** and **complex 3** recorded in dichloromethane at room temperature.

spectra of the **complexes 1, 2 and 3** show strong absorption bands in dichloromethane at $\lambda = 1007$ nm ($\epsilon \sim 34\,000$ L mol⁻¹ cm⁻¹), $\lambda = 1010$ nm ($\epsilon \sim 34\,000$ L mol⁻¹ cm⁻¹) and $\lambda = 1007$ nm ($\epsilon \sim 38\,000$ L mol⁻¹ cm⁻¹), respectively. Their absorption bands are offset to the NIR region in comparison to analogues substituted by phenyl rings.^{7–9,20} We observe a minor solvatochromic effect as their absorption is shifted by only 15 nm towards lower wavelengths in heptanes, in comparison with dichloromethane. The three complexes exhibit relatively low absorption from 450 to 700 nm. For the three complexes, the optical bandgaps measured in solution are equal to 1.15 eV. Thin films of **complexes 1 and 2** present enlarged absorption bands (in comparison with solutions) leading to a slightly lower value of 1.08 eV. **Complex 3** did not give rise to reliable data on thin films for film quality reasons.

Raman spectroscopy and computed Raman data

Resonance Raman excitation profiles have been determined for crystals of **complex 1** and **complex 3** and for an oil of **complex 2** in the 200–1500 nm region. These spectra (Fig. 8) are fairly similar to those obtained for the [Ni(S₂C₂S₂)₂] core of neutral bis(1,2-dithiolene) complexes.^{21,22} For **complex 3**, two distinct low frequency bands are observed at 382 cm⁻¹ and 372 cm⁻¹ (see Fig. 8, top) whereas a single signal is observed in this region for the two other compounds.

We have calculated Raman modes and assigned their respective representations to bands vibrations (see ESI†, Fig. S5). The spectral features for the three compounds are quite similar. Due to interaction with neighbouring molecules in the crystal state, some deviation from the calculated frequencies of the free complexes is expected for **complex 1** and **complex 3**. Analysis of vibration modes of **complex 2** is more difficult due to the lack of molecular symmetry. It is anticipated that the oily nature of **complex 2** may induce a great variety of lateral chain conformations. This is probably the reason why the Raman spectrum of **complex 2** displays numerous poorly resolved bands. For both **complexes 1 and 3**, the Raman spectra have a limited number of vibration modes because of the rule of mutual exclusion. Only molecular vibrations symmetric with regard to the centre of symmetry (symmetry A_g) are present. Among them we find characteristic modes of the core of these complexes.

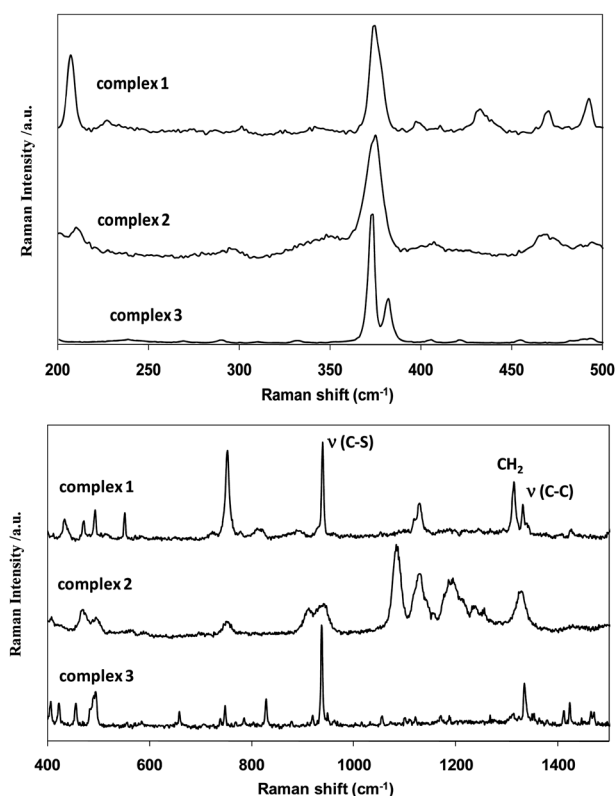


Fig. 8 Raman spectra of **complexes 1, 2 and 3** (a) in the 200–500 nm region (top) and (b) in the 400–1500 nm region (bottom).

Fundamental vibrations of the nickel core are weakly influenced by the presence of alkyl chains. The low frequency band near 380 cm^{-1} corresponds to a combination of Ni–S stretching bond and C=C–S bending modes. In the case of **complex 3**, an additional band is observed. As shown in Fig. S-5 (see ESI†), it could be attributed to a combination of symmetric Ni–S bond stretching with C–CMe–C bending. As expected, the intense band near 985 cm^{-1} corresponds to the C–S bond stretching mode. The weak intense mode at 1393 cm^{-1} corresponds to the C–C stretching mode.

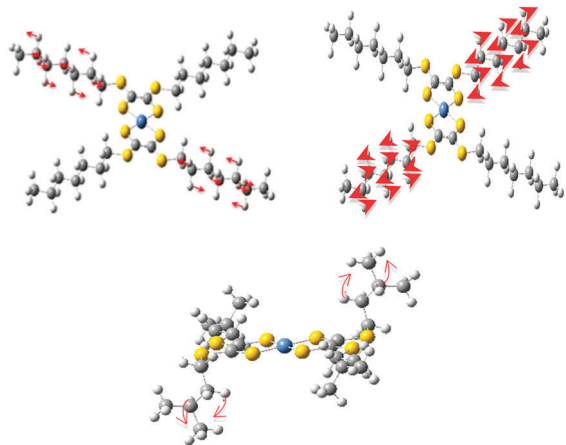


Fig. 9 Normal vibrations of the alkyl chains of **complex 1**: CH₂ twisting mode at 1323 cm^{-1} (top left); CH₂ twisting mode at 1325 cm^{-1} (top right) and **complex 3**: C–C–C bending mode at 1334 cm^{-1} (bottom).

This value is exactly the same for the three complexes, maybe because this mode is not mixed with other vibrations.

Fig. 9 displays selected normal vibrations of the different alkyl chains. Calculated values for H–C–H, H–C–C and C–C–C bending motions occur in the $1000\text{--}1500\text{ cm}^{-1}$ region. For instance, **complex 1** shows twisting modes of the CH₂ group with frequencies of 1322 cm^{-1} , 1323 cm^{-1} and 1325 cm^{-1} . Theoretical calculations predict an increase in the vibration intensity per added CH₂ group. Experimental results confirm this prediction. In **complex 3**, the frequency of 1334 cm^{-1} is attributed to the bending of the C–CMe–C linkage. Agreement between theoretical and experimental data appears satisfactorily good and our assignments are in accordance with those proposed for other neutral bisdithiolene complexes in recent work.²³

Experimental

Synthetic procedures

All solvents used were dried by refluxing over magnesium turnings, followed by distillation, and then stored under argon before use.

Preparation of [Ni(S₂C₂(SC₇H₁₅)₂)] 1. Sodium methanolate freshly prepared from 0.23 g of sodium (10 mmol) dissolved in dry methanol was added under a dry argon atmosphere to a solution of 4,5-bis(benzoylthio)-1,3-dithiole-2-thione (2.00 g, 4.92 mmol) in methanol (10 mL). After 1 h of stirring, 1.6 mL of 1-bromoheptane (1.82 g, 10 mmol) was added dropwise to the dark purple solution. The mixture was then refluxed ($78\text{ }^{\circ}\text{C}$) for 5 h, under vigorous agitation. The dark orange solution was concentrated *in vacuo* to afford an orange oil. Addition of pentane (20 mL) to this oil induced a white solid to precipitate (NaBr), which was filtered and washed with pentane (10 mL). The collected filtrates were concentrated under vacuum and the resulting orange oil was purified by a chromatography column (silica gel Fluka 60, eluant: hexane–acetone (95/5)) to afford 1.93 g of **ligand 1** (quantitative yield) as a pale yellow oil. ¹H NMR (CD₂Cl₂) δ , ppm: 0.92 (t, 6H, ³J(H,H) = 6.7 Hz), 1.32 to 1.47 (m, 16H), 1.70 (q, 4H, ³J(H,H) = 7.5 Hz), 2.92 (t, 4H, ³J(H,H) = 7.5 Hz); GCMS: $m/z = 394\text{ (M}^+)$.

Pentane-washed sodium (0.23 g, 10 mmol) dissolved in methanol (10 mL) was added to the preceding oil (4.9 mmol) dissolved in 10 mL of dry methanol. The orange mixture was refluxed ($78\text{ }^{\circ}\text{C}$) for 2.5 h under vigorous stirring and then allowed to cool to room temperature. A solution of [Bu₄N][Br] (3.22 g, 10 mmol) in methanol (10 mL) was added. After 1 h of stirring, NiCl₂·6H₂O (0.59 g, 2.5 mmol) in methanol (50 mL) was added dropwise. The mixture was then maintained at room temperature overnight with stirring. After filtration of the mixture, the solvent was removed under vacuum to yield a black-brown oily solid which was redissolved in acetone (50 mL).

To the dark brown solution was added I₂ (0.63 g, 2.5 mmol) and NaI (1.12 g, 7.5 mmol) dissolved in acetone (40 mL), resulting in an instantaneous colour change to dark green. Reduction of the solvent volume induced a dark coloured solid

to precipitate, which was filtered off, washed with methanol and dried.

Recrystallisation from CH_2Cl_2 – IprOH afforded the pure dark green crystalline product (0.62 g, yield 33%); mp 82 °C. IR (KBr) ν , cm^{-1} : 490 (NI–S), 803 (C–S), 1020, 1098, 1257 (C–C) + (C–S), 1418 (C=C); near-IR absorption spectrum (CH_2Cl_2) λ_{max} , nm (ϵ_{M} , $\text{L mol}^{-1} \text{cm}^{-1}$): 1007 (33 600); $^1\text{H NMR}$ (CD_2Cl_2) δ , ppm: 0.93 (t, 12H, $^3J(\text{H,H}) = 6.9$ Hz), 1.35 to 1.57 (m, 32H), 1.88 (m, 8H), 3.42 (m, 8H); Raman spectrum (on crystal) ν , cm^{-1} : 230 (m), 380 (s), 440 (w), 478 (w), 495 (w), 508 (w), 555 (w), 940 (m), 1065 (w), 1316 (s), 1332 (s) and 1411 (m); anal calc. for $\text{C}_{32}\text{H}_{60}\text{S}_8\text{Ni}$: C, 50.57; H, 7.96; S, 33.75; Ni, 7.72%. Found: C, 50.45; H, 7.93; S, 34.02; Ni, 7.76%.

Preparation of $[\text{Ni}(\text{S}_2\text{C}_2(\text{SC}_5\text{H}_{17})_2)_2]$ 2. The neutral complex 2 was prepared in the same way. The ligand 2 was first synthesized, purified by a chromatography column (silica gel Fluka 60, eluant: hexane–dichloromethane (90/10)) and isolated as a yellow oil in quantitative yield (2.07 g); $^1\text{H NMR}$ (CD_2Cl_2) δ , ppm: 0.92 (m, 12H), 1.29 to 1.55 (m, 16H), 1.55 to 1.67 (m, 2H), 2.92 (d, 4H, $^3J(\text{H,H}) = 6.3$ Hz); GCMS: $m/z = 422$ (M^+). It was then totally engaged in the synthesis of the green oily complex 2, which was purified by a chromatography column (silica gel Fluka 60, eluant: hexane–dichloromethane (99/1)); (1.4 g, yield 69%); near-IR absorption spectrum (CH_2Cl_2) λ_{max} , nm (ϵ_{M} , $\text{L mol}^{-1} \text{cm}^{-1}$): 1010 (33 600); $^1\text{H NMR}$ (CD_2Cl_2) δ ppm: 0.93 to 0.99 (m, 24H), 1.30 to 1.61 (m, 32H), 1.88 (m, 4H), 3.42 (m, 8H); anal calc. for $\text{C}_{36}\text{H}_{68}\text{S}_8\text{Ni}$: C, 52.98; H, 8.40; S, 32.01; Ni, 7.19%. Found: C, 53.30; H, 8.41; S, 31.14; Ni, 6.84%.

Preparation of $[\text{Ni}(\text{S}_2\text{C}_2(\text{SC}_5\text{H}_{11})_2)_2]$ 3. The neutral complex 3 was prepared in the same way. The ligand 3 was first synthesized, purified by a chromatography column (silica gel Fluka 60, eluant: hexane–dichloromethane (95/5)) and isolated as a yellow oil in quantitative yield (1.80 g); $^1\text{H NMR}$ (CD_2Cl_2) δ , ppm: 0.95 (d, 12H, $^3J(\text{H,H}) = 6.6$ Hz), 1.55 to 1.63 (m, 2H), 1.73 to 1.76 (m, 4H), 2.91 to 2.96 (m, 4H); GCMS: $m/z = 338$ (M^+). It was then totally engaged in the synthesis of complex 3, which was purified by recrystallisation from hexane–acetone to give the pure dark green crystalline product (1.0 g, 52%); mp 168 °C; IR (KBr) ν/cm^{-1} : 490 (NI–S), 803 (C–S), 1020, 1098, 1257 (C–C) + (C–S), 1418 (C=C); near-IR absorption spectrum (CH_2Cl_2) λ_{max} , nm (ϵ_{M} , $\text{L mol}^{-1} \text{cm}^{-1}$): 1007 (37 600); $^1\text{H NMR}$ (CD_2Cl_2) δ , ppm: 1.02 (d, 24H, $^3J(\text{H,H}) = 6.6$ Hz), 1.55 (s, 4H), 1.76 to 1.81 (m, 8H), 3.40 to 3.46 (t, 8H, $^3J(\text{H,H}) = 7.5$ Hz); anal calc. for $\text{C}_{24}\text{H}_{44}\text{S}_8\text{Ni}$: C, 44.50; H, 6.84; S, 39.60; Ni, 9.06%. Found C, 44.19; H, 6.75%; S, 39.37%; Ni, 8.66%.

Chemical analyses

GCMS analysis was realised on a Hewlett Packard 6890 CPG combined with a Hewlett Packard 5973 mass spectrometer.

Physical measurements

IR spectra and near-infrared spectra were recorded on a Perkin Elmer GX FT-IR spectrophotometer. Raman measurements were carried out at room temperature using a Raman

spectrometer (DYLOR XY micro Raman) equipped with a helium–neon laser ($\lambda = 6328$ Å, laser power density: 9×10^4 W cm^{-2}). $^1\text{H NMR}$ spectra were recorded on a Bruker DPX 300 spectrometer operating at 300.13 MHz. Dichloromethane- d^2 (CD_2Cl_2) was used as the solvent and tetramethylsilane (TMS) as the internal standard. Melting points were determined by DSC thermograms obtained on a DSC 204 NETZSCH system using 2–5 mg samples in 30 μl sample pans and a scan rate of 10 °C min^{-1} . Mass analyses were performed at the MS Service of the Paul Sabatier University. Elemental analyses were carried out at the CNRS Central Analyses Service in Lyon. Electronic spectra were recorded on a Perkin Elmer Lambda 35.

Voltammetric measurements were carried out with an Autolab PGSTAT100 potentiostat controlled by GPES 4.09 software. Experiments were performed at room temperature in a homemade airtight three-electrode cell connected to a vacuum/argon line. A saturated calomel electrode (SCE) separated from the solution by a bridge compartment was used as a reference electrode. The counter electrode was a platinum wire of ca. 1 cm^2 apparent surface. Working electrodes were: a Pt microdisk (0.5 mm diameter). The supporting electrolyte, ($n\text{-Bu}_4\text{N}$)[PF₆] (Fluka, 99% puriss electrochemical grade), was used as received. For studies in solution, electrochemical media containing 0.1 mol L^{-1} of supporting electrolyte, and 10^{-3} mol L^{-1} of complex were used. Before each measurement, the solutions were deaerated by bubbling argon and the working electrode was polished with a Presi P230 polishing machine. Square Wave Voltammetry (SWV) was performed at room temperature, and the parameters are: SW frequency $f = 20$ Hz, SW amplitude $E_{\text{SW}} = 20$ mV, and scan increment $dE = 5$ mV.

Structure determination

Single-crystal X-ray diffraction data were collected at 160 K for complex 1 and at 150 K for complex 3 on a Xcalibur Oxford Diffraction diffractometer using graphite-monochromated Mo K α radiation. Crystals were cooled by a nitrogen gas flow using an Oxford Cryosystems Cryostream Cooler Device. The structures were solved by direct methods using SIR92,²⁴ and refined by means of least-squares procedures on F using the programs of the PC version of CRYSTALS.²⁵ Atomic scattering factors were taken from the International Tables for X-ray Crystallography.²⁶ All non-hydrogen atoms were refined anisotropically. Hydrogen atoms were located on difference Fourier maps and repositioned geometrically during the refinement process using the riding model. The programs MERCURY,²⁷ ORTEP III²⁸ and CAMERON²⁹ were used for drawings.

Crystal structure determination of complex 1 at 160 K

Crystal data. $\text{C}_{32}\text{H}_{60}\text{Ni}_1\text{S}_8$, $M = 760.07$, triclinic, $a = 5.3358(6)$ (Å), $b = 13.3538(13)$ (Å), $c = 13.8940(18)$ (Å), $\alpha = 101.260(10)^\circ$, $\beta = 90.396(10)^\circ$, $\gamma = 101.111(19)^\circ$, $V = 951.72(19)$ (Å)³, $T = 160$ K, space group $P\bar{1}$, $Z = 1$, $\mu(\text{MoK}\alpha) = 2.463$, 9034 reflections measured, 5044 independent reflections ($R_{\text{int}} = 0.06$) of which 1929 reflections with $I > 1.7\sigma(I)$ were used for the refinement of 187 parameters. The final R and $wR(F)$ are 0.046 and 0.051, respectively.

Crystal structure determination of complex 3 at 150 K

Crystal data. C₂₄H₄₄Ni₁S₈, *M* = 647.85, monoclinic, *a* = 26.182(2) (Å), *b* = 6.4642(6) (Å), *c* = 19.9353(11) (Å), β = 107.729(6)°, *V* = 3213.7(5) (Å)³, *T* = 150 K, space group *C2/c*, *Z* = 4, $\mu(\text{MoK}\alpha)$ = 2.463, 30 379 reflections measured, 4287 independent reflections (*R*_{int} = 0.04) of which 2201 reflections with *I* > 3 σ (*I*) were used for the refinement of 151 parameters. The final *R* and *wR*(*F*) are 0.032 and 0.036, respectively.

Calculations

Two different procedures were applied depending on the complexes.

Complex 1 and complex 3. Calculations were performed using the *Gaussian 03* package. The PBE0³⁰ functional was used to perform geometry optimisations followed by analytical Raman frequency calculations.

Starting from crystallographic data, geometry optimization led to an electronic structure of C_i symmetry. Raman frequencies were determined *via* DFT using the PBE0 functional. Calculations are performed with a triple- ζ plus polarisation basis set (6-311G, (2df, 2pd))³¹ for the hydrogen and carbon atoms, a sulfur atom is described with a triple- ζ plus polarisation basis set (6-311++G, (3df, 3pd)).³² The inner 10 core electrons of the Ni atom were described using the Stuttgart relativistic effective core potential with the corresponding basis set (6s5p3d1f).³³

Complex 2. Due to the size of this complex and in the absence of crystallographic data another strategy was used to study **complex 2**. Electronic structure calculations and Raman frequency calculations of **complex 2** were carried out with PC Gamess.³⁴ Geometry optimizations and Raman frequency analyse were run without symmetry constraints. The PBE0 functional was employed in combination with scalar relativistic core potential SBKJC and their corresponding basis sets³⁵ for all atoms.

For comparison purposes, data proposed in Fig. 6 were obtained from a single point energy calculation with the same procedure as that used for the **complexes 1 and 3**.

Prediction of Raman intensities. The Raman activities (*S*_{*i*}) calculated were converted to relative Raman intensities (*I*_{*i*}) using the following relationship derived from the basic theory of Raman scattering.³⁶

$$I_i = \frac{f(\bar{\nu}_0 - \bar{\nu}_i)^4 S_i}{\bar{\nu}_i [1 - \exp(-hc\bar{\nu}_i/kT)]}$$

where $\bar{\nu}_0$ is the exciting frequency (in cm⁻¹), $\bar{\nu}_i$ is the vibrational wavenumber of the *i*th mode, *h*, *c* and *k* are the fundamental constants and *f* is a suitably chosen common normalization factor for all peak intensities. Herein the conversion was carried out with $\bar{\nu}_0 = 15802.8$ cm⁻¹ and *T* = 298 K.

The Raman frequencies were not corrected for anharmonicity or other additional effects by scaling factors.

Conclusions

Three neutral nickel complexes of the “non-cyclic SR” family have been investigated and fully characterized. Their crystalline organization, their behaviour in electrochemistry and their electronic spectra (UV-vis and Raman) were fully investigated. The nature of the alkyl chains has no influence on the electronic properties, *i.e.* electrochemistry and electronic spectra (UV-vis and Raman) of the three investigated complexes but shows significant impact on the physical properties, *i.e.* melting point and crystalline organization. All the experimental data were systematically discussed in the light of computed values. Using these theoretical tools, we show a direct link between measured and calculated molecular parameters and we demonstrate the accuracy of theoretical calculations for these three neutral nickel coordination compounds. This reinforces our wish to combine experimental and theoretical approaches and encourages us to continue in this way. This approach opens the way toward predictive calculations, a very ambitious topic in the field of organic electronics. Further works will concern the design of such molecules for organic electronics, with a new challenge that consists of taking into account charge transfer considerations.

Acknowledgements

The authors thank French National Research Agency for financial support as part of ANR CPA-FALOIR 2007–2010 and ANR Spir-Wind 2009–2012 Projects. The authors also thank Professor Colin J. Marsden for critically reading the manuscript.

References

- 1 Y. Wen and Y. Liu, *Adv. Mater.*, 2010, **22**, 1331.
- 2 L. Duan, J. Qiao, Y. Sun and Y. Qiu, *Adv. Mater.*, 2011, **23**, 1137.
- 3 S. Shanmugaraju, S. A. Joshi and P. S. Mukherjee, *Inorg. Chem.*, 2011, **50**, 11736.
- 4 (a) T. M. Clarke and J. R. Durrant, *Chem. Rev.*, 2010, **110**, 6736; (b) D. Credgington, R. Hamilton, P. Atienzar, J. Nelson and J. R. Durrant, *Adv. Funct. Mater.*, 2011, **21**, 2744.
- 5 A. Weston and M. Murthy, *Carbon*, 1996, **34**, 1267.
- 6 J. E. Antony, *Chem. Mater.*, 2011, **23**, 583.
- 7 T. T. Bui, B. Garreau-de Bonneval and K. I. Moineau-Chane Ching, *New J. Chem.*, 2010, **34**, 337.
- 8 T. T. Bui, O. Thiebaut, E. Grelet, M. F. Achard, B. Garreau-de Bonneval and K. I. Moineau-Chane Ching, *Eur. J. Inorg. Chem.*, 2011, **17**, 2663.
- 9 J.-Y. Cho, B. Domercq, S. C. Jones, J. Yu, X. Zhang, Z. An, M. Bishop, S. Barlow, S. R. Marder and B. Kippelen, *J. Mater. Chem.*, 2007, **17**, 2642.
- 10 B. Garreau-de Bonneval, K. I. Moineau-Chane Ching, F. Alary, T. T. Bui and L. Valade, *Coord. Chem. Rev.*, 2010, **254**, 1457 and references therein.
- 11 G. Soras, N. Psaroudakis, M. J. Manos, A. J. Tasiopoulos, D. G. Liakos and G. A. Mousdis, *Polyhedron*, 2009, **28**, 3340.
- 12 F. Alary, J. L. Heully, A. Scemama, B. Garreau-de-Bonneval, K. I. Chane-Ching and M. Caffarel, *Theor. Chem. Acc.*, 2010, **126**, 243 and references therein.
- 13 A. Charlton, C. A. S. Hill, A. E. Underhill, K. M. A. Malik, M. B. Hursthouse, A. I. Karaulov and J. Moller, *J. Mater. Chem.*, 1994, **4**, 1861.
- 14 A. Sournia-Saquet, B. Garreau-de Bonneval, K. I. Chane-Ching and L. Valade, *J. Electroanal. Chem.*, 2008, **624**, 84.
- 15 J. L. Brédas, R. Silbey, D. S. Boudreaux and R. R. Chance, *J. Am. Chem. Soc.*, 1983, **105**, 6555.
- 16 U. T. Mueller-Westerhoff, B. Vance and D. I. Yoon, *Tetrahedron*, 1991, **47**, 909.

- 17 F. Bigoli, P. Deplano, F. A. Devillanova, V. Lippolis, P. J. Lukes, M. L. Mercuri, M. A. Pellinghelli and E. F. Trogu, *J. Chem. Soc., Chem. Commun.*, 1995, 371.
- 18 F. Bigoli, P. Deplano, M. L. Mercuri, M. A. Pellinghelli, G. Pintus, E. F. Trogu, G. Zonnedda, H. H. Wang and J. M. Williams, *Inorg. Chim. Acta*, 1998, **273**, 175.
- 19 C. L. Kean, D. O. Miller and P. G. Pickup, *J. Mater. Chem.*, 2002, **12**, 2949.
- 20 P. Basu, A. Nigam, B. Mogesa, S. Denti and V. N. Nemykin, *Inorg. Chim. Acta*, 2010, **363**, 2857.
- 21 *Dithiolene chemistry Synthesis, Properties and Applications*, Prog. Inorg. Chem. 52, ed. E. I. Stiefel, J. Wiley and Sons, Hoboken, New Jersey, 2004.
- 22 K. I. Pokhodnya, C. Faulmann, I. Malfant, R. Andreu-Solano, P. Cassoux, A. Mlayah, D. Smirnov and J. Leotin, *Synth. Met.*, 1999, **103**, 2016.
- 23 O. Siimann and J. Fresco, *Inorg. Chem.*, 1971, **10**, 297.
- 24 A. Altomare, G. Cascarano, C. Giacovazzo and A. Guagliardi, *J. Appl. Crystallogr.*, 1993, **26**, 343.
- 25 P. W. Betteridge, J. R. Carruthers, R. I. Cooper, K. Prout and D. J. Watkin, *J. Appl. Crystallogr.*, 2003, **36**, 1487.
- 26 D. T. Cromer, *International Tables for X-ray Crystallography*, the Kynoch Press, Birmingham, England, vol. IV, 1974.
- 27 Copyright © 2005 The Cambridge Crystallographic Data Centre, Registered Charity No 800579.
- 28 M. N. Burnett and C. K. Johnson, *ORTEP III, Report ORNL-6895*, Oak Ridge National Laboratory, Tennessee, USA, 1996.
- 29 D. M. Watkin, L. Pearce and C. K. A. Prout, *CAMERON*, University of Oxford, England, 1993.
- 30 C. Adamo and V. Barone, *J. Chem. Phys.*, 1999, **110**, 6158.
- 31 R. Krishnan, J. S. Binkley, R. Seeger and J. A. Pople, *J. Chem. Phys.*, 1980, **72**, 650.
- 32 A. D. McLean and G. S. Chandler, *J. Chem. Phys.*, 1980, **72**, 5639.
- 33 M. Dolg, H. Stoll, H. Preuss and R. M. Pitzer, *J. Phys. Chem.*, 1993, **97**, 5852.
- 34 A.V. Nemukhin, B.L. Grigorenko, A.A. Granovsky, Molecular modeling by using the PC GAMESS program: From diatomic molecules to enzymes, *Moscow University Chemistry Bulletin*, 2004, **45**, 75.
- 35 W. J. Stevens, M. Krauss, H. Basch and P. G. Jasieu, *Can. J. Chem.*, 1992, **70**, 612.
- 36 P. L. Polavarapu, *J. Phys. Chem.*, 1990, **94**, 8106.